IEEE Photonics Journal
An IEEE Photonics Society Publication

Open Access

Collimation Sensing With Differential Grating and Talbot Interferometry

Volume 6, Number 3, June 2014

Nan Wang
Yan Tang
Wei Jiang
Wei Yan
Song Hu

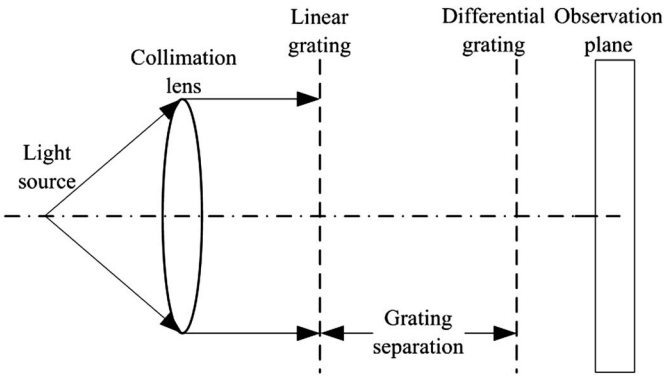

DOI: 10.1109/JPHOT.2014.2317678
1943-0655

Collimation Sensing With Differential Grating and Talbot Interferometry

Nan Wang,[1,2] Yan Tang,[1] Wei Jiang,[1] Wei Yan,[1] and Song Hu[1]

[1]State Key Laboratory of Optical Technologies for Microfabrication, The Institute of Optics and Electronics, Chinese Academy of Sciences, Chengdu 610209, China
[2]University of Chinese Academy of Sciences, Beijing 100039, China

DOI: 10.1109/JPHOT.2014.2317678

Manuscript received February 28, 2014; revised March 24, 2014; accepted March 28, 2014. Date of publication April 16, 2014; date of current version April 30, 2014. This work was supported by the National Natural Science Foundation of China under Grant 61274108 and Grant 61274114. Corresponding author: N. Wang (e-mail: 705679317@qq.com).

Abstract: The collimation of monochromatic light in optical metrology is of great importance for its determination of the accuracy of physical measurement. This paper proposes a novel collimation testing method with the differential grating (DG) characterized by its high sensitivity. In the process of measurement, the monochromatic light is incident upon a linear grating and is then projected onto a DG to create two sets of linear moiré fringes. By analyzing the relationship between the phase of moiré fringes and the divergence or convergence angle, the collimation of monochromatic light can be easily measured. Compared with the traditional collimation methods, this method is more accurate with an experimental accuracy of 10^{-7} rad, which is in good agreement with the theoretical prediction.

Index Terms: Collimation testing, moiré fringe, differential grating.

1. Introduction

The collimation of monochromatic light has an important influence on the accuracy in the optical metrology. Therefore, an easy and high-accuracy method to check the quality of monochromatic light is significant. Several collimation testing techniques based on the Talbot effect and moire technique have been published [1]–[12]. For example, in 1971, Silva reported the use of Talbot interferometry with linear gratings for collimation testing [1]. Then, a dual-field grating with self-referencing capability and higher sensitivity was introduced by Kothiyal and Sirohi [5]. Shortly after, a study on collimation testing using spiral gratings was reported by Chang and Su [6]. In their paper, authors also pointed that the resultant moiré fringes of linear gratings are in linear distribution, leading to inconvenience to distinguish the state of collimation clearly. In 1994, Sriram carried out a comparative study on collimation testing with the dual-field linear, spiral and evolute grating [8]. It established that, of these three kinds of grating, the dual field grating exhibits the highest sensitivity for collimation testing. In 2008, the Fourier-transform algorithm (FTA) and the spatial phase-shifting algorithm (SPSA) were jointly proposed to determine the phase distribution of the dual-spiral moire fringes by Huang and Su [10]. The results showed that the FTA and SPSA are theoretically precise, effective and insensitive to the random noise, but this scheme is not verified by the experiment. In the same year, Shakher and co-workers reported their investigation on collimation testing with circular gratings [3]. Its result revealed that the sensitivity is better than dual-field gratings scheme. However,

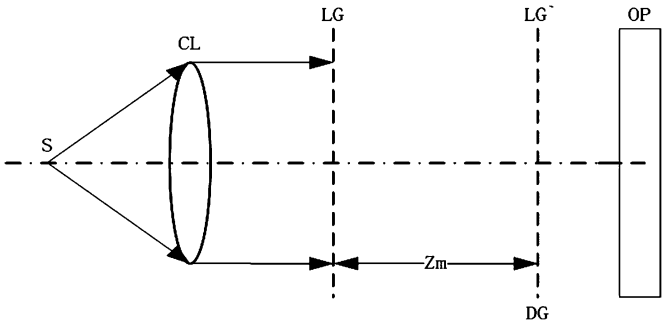

Fig. 1. Optical arrangement for the collimation test: the light source S, the collimation lens CL, the observation plane OP, and the grating separation Z_m.

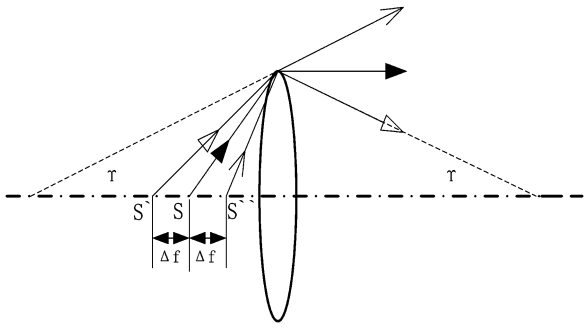

Fig. 2. Relationship between $\Delta\gamma$ and Δf.

the quantitative measurement cannot be achieved, making it not suit for the engineering applications.

In summary, those methods above cannot possess two merits below simultaneously:

- The resultant moiré fringes are convenient to measure qualitatively and quantitatively.
- The method has a high accuracy.

Herein, a collimation method based on the differential grating is proposed. In this method, the self-image of linear grating is projected on a differential grating. Because of the specifically designed grating pitches, the resultant moiré fringes are divided into two parts (the upper one and the lower one), in which moiré fringes have the same phase distribution in the case of the collimated light. When the collimation is disturbed, the period of resultant moiré fringes is magnified in one part and demagnified in the other part. This design can improve the sensitivity to a great degree and make the result simple to check. According to the experimental result, the divergence or convergence angle of 10^{-7} rad can be readily measured.

This paper is arranged as follows. In Section 2, the relationship between the divergence or convergence angle and the phase of moiré fringes is analyzed. Next, the simulational and experimental results are given to verify the proposed method. Finally, the results and applications are simply discussed.

2. Theoretical Models

The optical arrangement is shown in Fig. 1. A beam of monochromatic light is incident upon the linear grating LG and then projected onto the differential grating DG, which is positioned at the Talbot self-image LG′ of LG. When the collimating lens is defocused, the plane monochromatic wave becomes spherical (diverging or converging), as shown in Fig. 2. The divergence or convergence angle γ of monochromatic light is related to the defocusing distance Δf as follows:

$$\tan\gamma = \frac{h\Delta f}{f(f-\Delta f)} \tag{1}$$

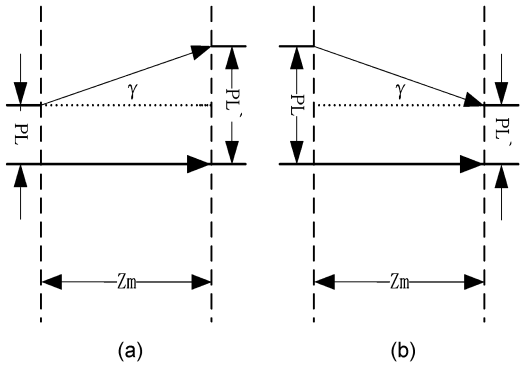

Fig. 3. Sketch map to determine the divergence or convergence angle γ. (a) Divergence angle. (b) Convergence angle.

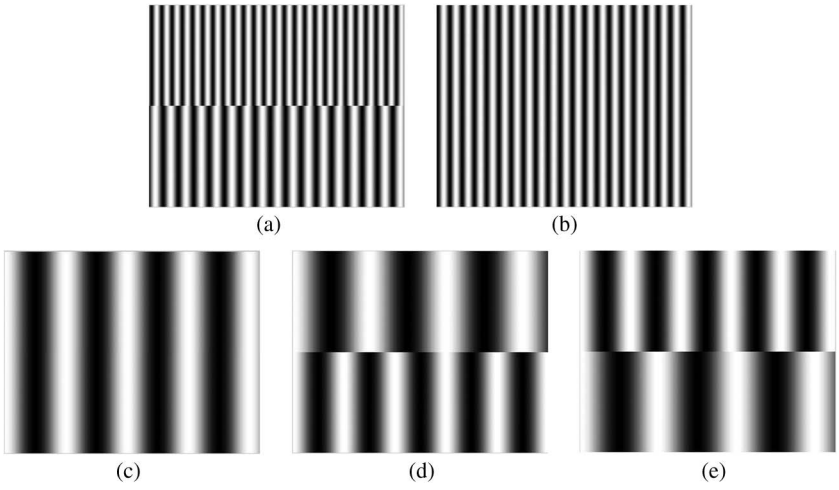

Fig. 4. The two group grating marks and the corresponding fringe. (a) Differential grating DG, (b) linear grating LG, (c) the fringe distribution of quasi-collimated light, (d) the fringe distribution of convergent light, and (e) the fringe distribution of divergent light.

where h is the height above the axis at which the incident ray strikes the collimating lens, and f is the focal length of the collimating lens.

In such a case, the self-image of LG becomes magnified or demagnified (as shown in Fig. 3), depending on whether the collimating lens is in focus or out of focus. The divergence or convergence angle is given as

$$\tan\gamma = \frac{P_l' - P_l}{Z_m} \tag{2}$$

where Z_m is the grating separation, and P_l and P_l' represent the pitch of LG and LG′, respectively. Since P_l and Z_m are determined by the experiment, the problem now is how to extract the characteristic parameter P_l'.

The LG and DG are illustrated in Fig. 4(a) and (b), respectively. The DG is comprised of two sets of line gratings. The upper line grating has the pitch P_{du} while the lower grating has the pitch P_{dd}. P_{dd} is closely equal to P_{du} plus an additional term $\Delta P(>0)$, that is, $P_{dd} = P_{du} + \Delta P$. The LG consists of one set of line grating with pitch P_l. Specifically, P_l is set as: $P_l = P_{dd}\ P_{du}/(P_{dd} + P_{du})$. For simplicity, let the amplitude transmittances of LG, DG_u, DG_d, and LG′ be written as

$$t_i(x) = \frac{1}{2} + \frac{1}{2}\cos\left(\frac{2\pi}{P_i}x + \theta_0\right) \tag{3}$$

where P_i represents the pitch of LG, DG_u, DG_d or LG′ when replaced by P_l, P_{du}, P_{dd} or P'_l. When the LG is projected onto the DG, the equivalent amplitude transmittance generated can be given as follows:

for the DG_u

$$\begin{aligned} t_u(x) &= t'_l(x)t_{du}(x) \\ &= \frac{1}{4} + \frac{1}{4}\cos\left(\frac{2\pi}{P'_l}x + \theta_0\right) + \frac{1}{4}\cos\left(\frac{2\pi}{P_{du}}x + \theta_0\right) \\ &\quad + \frac{1}{8}\cos\left[\left(\frac{2\pi}{P_{du}} - \frac{2\pi}{P'_l}\right)x\right] + \frac{1}{8}\cos\left[\left(\frac{2\pi}{P_{du}} + \frac{2\pi}{P'_l}\right)x + 2\theta_0\right] \end{aligned} \tag{4}$$

for the DG_d

$$\begin{aligned} t_d(x) &= t'_l(x)t_{dd}(x) \\ &= \frac{1}{4} + \frac{1}{4}\cos\left(\frac{2\pi}{P'_l}x + \theta_0\right) + \frac{1}{4}\cos\left(\frac{2\pi}{P_{dd}}x + \theta_0\right) \\ &\quad + \frac{1}{8}\cos\left[\left(\frac{2\pi}{P'_l} - \frac{2\pi}{P_{dd}}\right)x\right] + \frac{1}{8}\cos\left[\left(\frac{2\pi}{P_{dd}} + \frac{2\pi}{P'_l}\right)x + 2\theta_0\right]. \end{aligned} \tag{5}$$

The difference-frequency components in Eqs. (4) and (5) contain the information of collimation. Therefore, the phases of difference-frequency components are extracted by the use of FTA [10], [12], [13]. The difference between them *can* be given as follows:

$$\Delta\varphi = \varphi_u - \varphi_d = 2\pi x\left(\frac{1}{P_{dd}} + \frac{1}{P_{du}} - \frac{2}{P'_l}\right). \tag{6}$$

From Eq. (6), P'_l can be deduced as

$$P'_l = \frac{4\pi}{2\pi(1/P_{dd} + 1/P_{du}) - d(\Delta\varphi)/dx}. \tag{7}$$

Substituted Eq. (7) into Eqs. (1) and (2). The small γ and Δf can be expressed as

$$\gamma = \frac{4\pi}{Z_m[2\pi(1/P_{dd} + 1/P_{du}) - d(\Delta\varphi)/dx]} - \frac{P_l}{Z_m} \tag{8}$$

$$\Delta f = \frac{f^2}{h}\left\{\frac{4\pi}{Z_m[2\pi(1/P_{dd} + 1/P_{du}) - d(\Delta\varphi)/dx]} - \frac{P_l}{Z_m}\right\}. \tag{9}$$

For the collimated light, $1/P'_l = 1/P_l = (P_{dd} + P_{du})/2$, then $\Delta\varphi = 0$, $\gamma = 0$, and $\Delta f = 0$. The two sets of moiré fringes are aligned (as shown in Fig. 4(c)) and the collimation of the beam is perfect.

For the divergent light, $1/P'_l < 1/P_l$, then $\gamma < 0$ and $\Delta f < 0$. The lower moiré fringes are closer and two sets of moiré fringes are staggered, as shown in Fig. 4(d). Because the light source is in focus, the collimated lens CL should be moved away from the light source.

For the convergent light, $1/P'_l > 1/P_l$, then $\gamma < 0$ and $\Delta f < 0$. As shown in Fig. 4(e), the upper moiré fringes are closer and two sets of moiré fringes are also staggered. Because the light source is out of focus, the collimated lens CL should be moved toward the light source.

3. Numerical Simulation

The numerical simulation is performed based on the theoretical model mentioned above. The pitches of DG and LG in the simulation are, respectively 4 μm (P_{du}), 6 μm (P_{du}). and 4.8 μm (P_l). A beam of monochromatic light with wavelength 632.8 nm is expanded by a 4× microscope objective and a pinhole of 6.6 μm diameter. Simultaneously, the separation between the two gratings (Z_m) is set as 7.428 mm.

TABLE 1

Mean values, standard deviations, and error percentages of the calculated γ with the noise level being 0.8 times the full intensity in 10 calculations

Lens Sample Number	Theoretical Value		Simulation		
	Δf (μm)	γ (10^{-6}rad)	$\bar{\gamma}$ (10^{-6}rad)	σ (10^{-8}rad)	Error percentages(%)
1	-500	-1.307	-1.333	1.167	1.99
2	500	1.333	1.362	1.241	2.18
3	-50	-0.1319	-0.1325	0.138	0.45
4	50	0.1321	0.1323	0.155	0.15

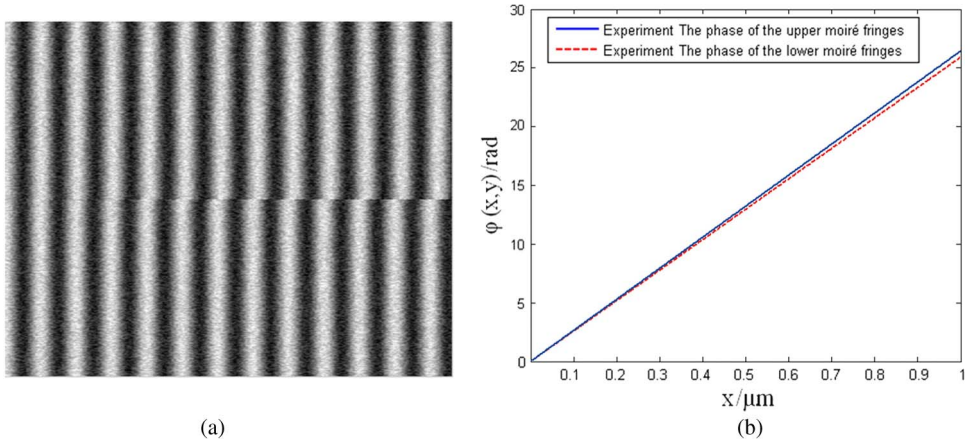

Fig. 5. Moiré fringe patterns in the simulation. (a) Moiré fringe patterns of convergent light with Δf of -500 μm. (b) $\varphi(x, y)$ against x by using FTA.

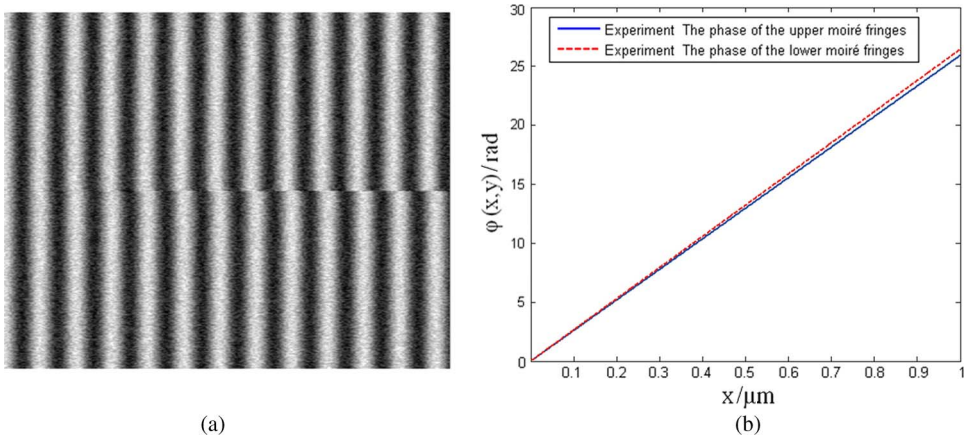

Fig. 6. Moiré fringe patterns in the simulation. (a) Moiré fringe patterns of divergent light with Δf of 500 μm. (b) $\varphi(x, y)$ against x by using FTA.

In the simulation, the random noise as 80% of the fringe patterns amplitude is added into the fringe patterns to calculate the divergence or convergence angle γ. To examine the accuracy of the proposed method, four groups of measurement are carried out with defocusing distances -500, 500, -50 and 50 μm, respectively. The mean values $(\bar{\gamma})$, standard deviations (σ) and error percentages of the calculated γ are shown in Table 1 while the corresponding moiré fringe patterns and phase distributions are given in Figs. 5–8. In the first group, the error percentage and standard

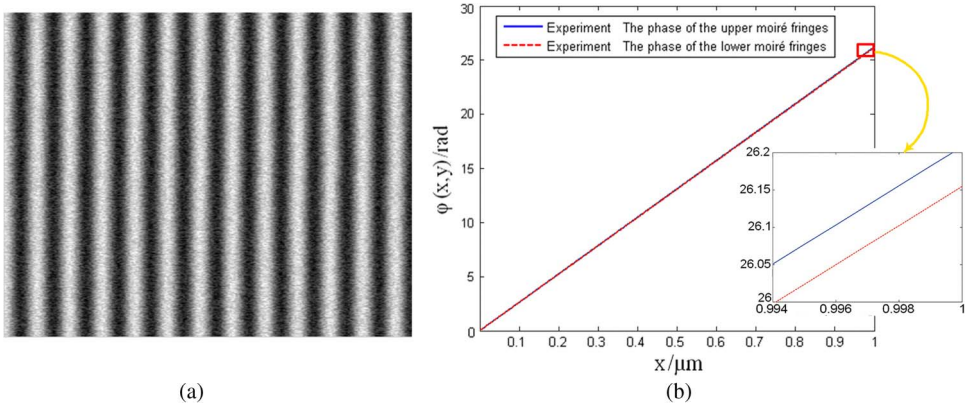

Fig. 7. Moiré fringe patterns in the simulation. (a) Moiré fringe patterns of convergent light with Δf of -50 μm. (b) $\varphi(x, y)$ against x by using FTA.

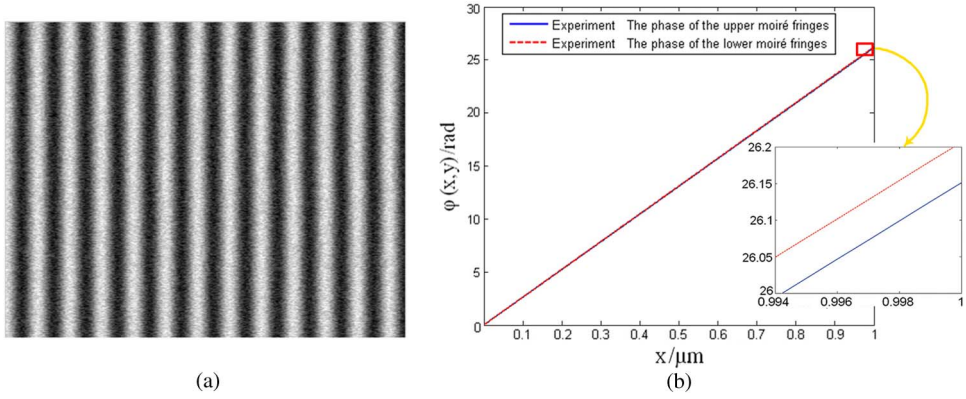

Fig. 8. Moiré fringe patterns in the simulation. (a) Moiré fringe patterns of divergent light with Δf of 50 μm. (b) $\varphi(x, y)$ against x by using FTA.

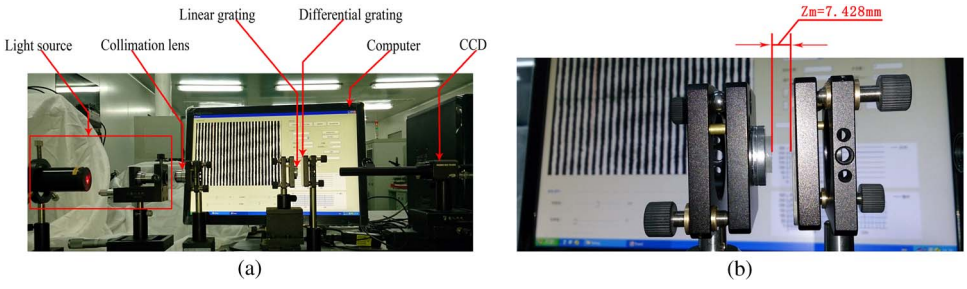

Fig. 9. (a) Experimental setup. (b) Grating separation is only 7.428 mm.

deviation of γ is 1.99% and 1.167e-008 rad, respectively. In the second group, the error percentage and standard deviation of γ is 2.18% and 1.241e-008 rad, respectively. In the third group, the error percentage and standard deviation of γ is 0.45% and 0.138e-008 rad, respectively. In the fourth group, the error percentage and standard deviation of γ is 0.15% and 0.155e-008 rad, respectively.

4. Experiment

The experimental setup is shown in Fig. 9. A He–Ne laser (25 LHR 151) with wavelength 632.8 nm and output power 5 mW, respectively, is used as the illumination source. The focal length and

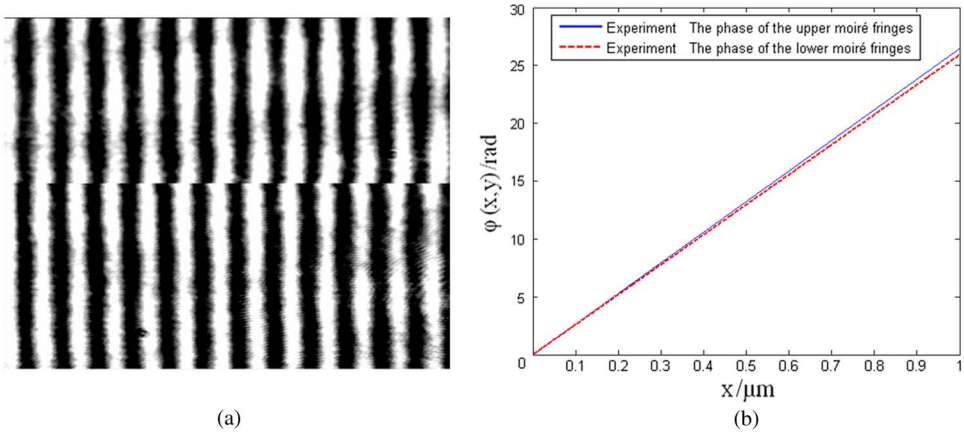

Fig. 10. Moiré fringe patterns in the experiment. (a) Moiré fringe patterns of convergent light with Δf of -500 μm. (b) $\varphi(x, y)$ against x by using FTA.

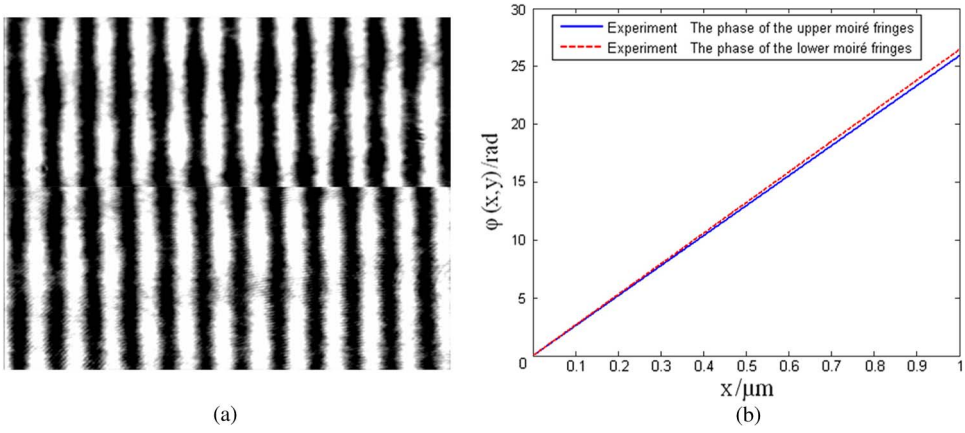

Fig. 11. Moiré fringe patterns in the experiment. (a) Moiré fringe patterns of divergent light with Δf of 500 μm. (b) $\varphi(x, y)$ against x by using FTA.

magnification of the collimation lens are, respectively 50 mm and 4×, and the diameter of pinhole is 6.6 μm. The CCD camera combined with a computer is used to capture the moiré fringe patterns. There is one differential grating used as DG, whose pitches are, respectively, 4 μm (P_{du}) and 6 μm (P_{dd}), and one line grating used as LG, whose pitch is 4.8 μm (P_l). They are designed by us and fabricated by the Institute of Microelectronics of Chinese Academy of Sciences (Beijing, China). In the experiment, the collimating lens is mounted upon a precision translation stage to translate the lens along the optic axis. The translation stage is driven by a micrometer screw with a reading precision of 1 μm. The lens position is adjusted to provide a collimated beam. The grating separation can be adjusted to set the required value of the Talbot plane at Z_m. The captured moire fringe patterns are processed by a computer using FTA.

In the experiment, the grating separation is adjusted to about 7.428 mm. When the LG and DG are adjusted to be parallel, two sets of linear moiré fringes are obtained. After that, the position of collimation is approached from either side (in focus or out of focus position) by the movement of the micrometer screw attached to the translation stage. This process continues until the two sets of moiré fringes are aligned, after which collimation is achieved. As soon as collimation is achieved, its position relative to the micrometer screw is recorded. The micrometer screw is rotated in the same or opposite direction until the collimation is just disturbed, and the position of the lens is again recorded. The difference between the two values is the defocusing distance. Four sets of

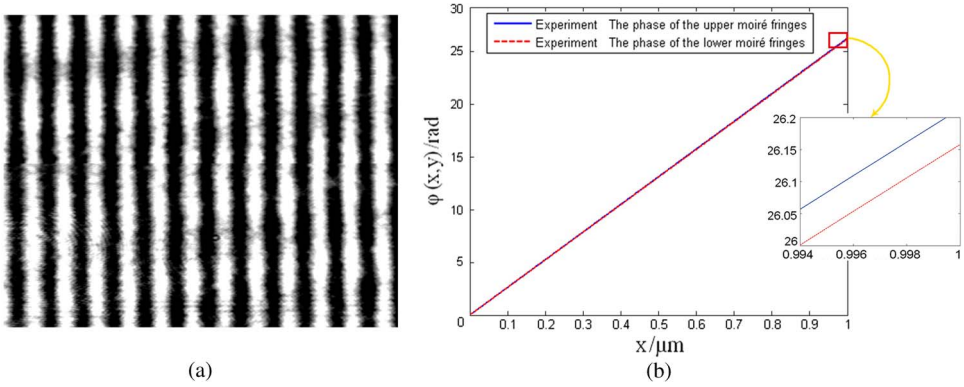

Fig. 12. Moiré fringe patterns in the experiment. (a) Moiré fringe patterns of convergent light with Δf of -50 μm. (b) $\varphi(x, y)$ against x by using FTA.

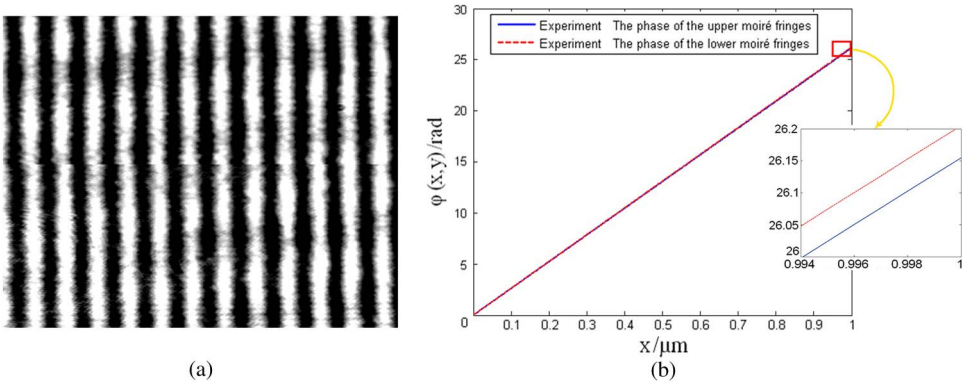

Fig. 13. Moiré fringe patterns in the experiment. (a) Moiré fringe patterns of divergent light with Δf of 50 μm. (b) $\varphi(x, y)$ against x by using FTA.

TABLE 2

Mean values, standard deviations and error percentages of the calculated γ with 10 times measurement

Lens Sample Number	Theoretical Value		Experiment		
	Δf (μm)	γ (10^{-6}rad)	$\bar{\gamma}$ (10^{-6}rad)	σ (10^{-8}rad)	Error percentages(%)
1	-500	-1.307	-1.340	1.485	2.52
2	500	1.333	1.367	2.014	2.55
3	-50	-0.1319	-0.1329	0.141	0.76
4	50	0.1321	0.1335	0.173	1.06

measurements are recorded. To improve the accuracy in phase extraction, the captured patterns are cut with integral number of moiré fringe period, as shown in Figs. 10–13. The mean values $(\bar{\gamma})$, standard deviations (σ) and error percentages of the γ are listed in Table 2. It can be seen that the error percentages are below 2.55%.

5. Discussions

The above simulational and experimental results indicate that the proposed method can achieve a measured accuracy of 10^{-7} rad level. By comparing Tables 1 with 2, its obvious that the experiment

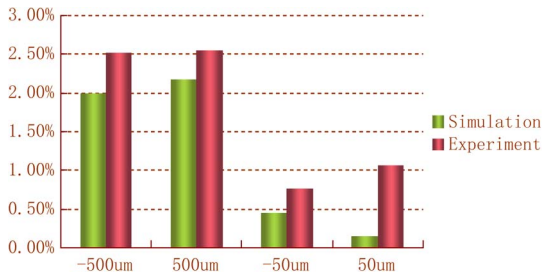

Fig. 14. Errors of γ in the simulation and experiment.

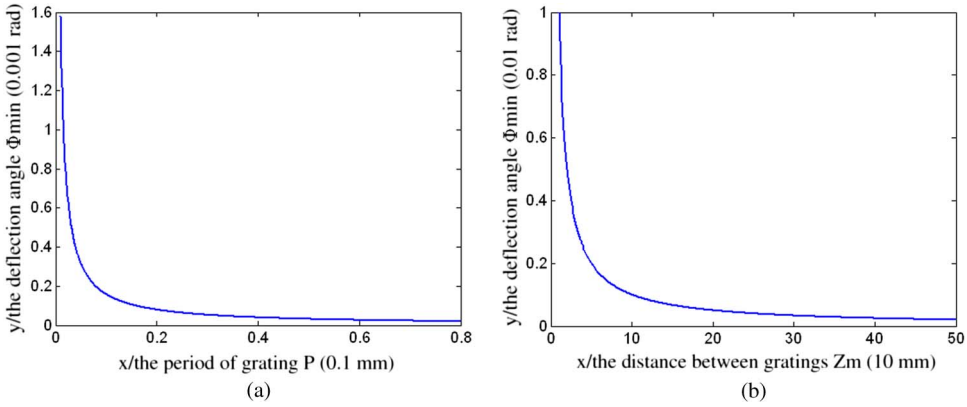

Fig. 15. Variations of the smallest detectable divergence or convergence angle Φ_{min} with (a) the grating pitch P and (b) the grating separation Z_m.

results are in good agreement with the simulation results, but the error ranges of γ in the experiment are larger than that in the simulation, as shown in Fig. 14. This is mainly caused by three reasons as follows.

1) The grating pitchs in the simulation are uniform, but not in the experiment. Because of the machining errors, the inconsistency of grating pitches influences the calculation of phase difference between two sets of fringes.
2) The phase distribution of moiré fringes correlates closely with the relative position between the LG and the DG. The relative angle between the LG and DG will lead to the tilt moiré fringes, which has an influence on the high-accuracy measurement because the extracted phase of tilt moiré fringes may inevitably lead to some errors [14], [15].
3) The noise in the experiment is more irregular than that in the simulation. In the simulation, only a randomly distributed Gaussian white noise is added, but the noise in practice is more complex and diverse, such as the speckle noise, CCD noise and environmental disturbance.

In practice, the smaller divergence or convergence angle (Φ_{min}) can be detected, the more sensitive the system is. The Φ_{min} is therefore a measure of sensitivity. The grating pitches in earlier studies are at the sub-millimeter level and good results are obtained with a long grating separation (at the decimeters or meters level). This is because the smallest detectable divergence or convergence angle increases with the decrease of grating pitch and grating separation, such as the experiment done by C. Shakher and co-workers. In their experiment, the results were obtained using the circular gratings with a pitch of 0.2 mm at several Talbot planes (250, 500, 750, 1000, 1250, 1500, and 1750 mm) [3]. And the relationships of the smallest detectable divergence or convergence angle with the grating pitch and grating separation are, respectively shown in Fig. 15(a) and (b). Therefore, it's a challenge to achieve high-precision results by adopting short grating pitch and grating separation. The proposed method in this paper is hopeful to solve these

deficiencies. Comparatively, in our experiment, the gratings with pitches of 4, 4.8 and 6 μm are used while the grating separation is only 7.428 mm. And the divergence or convergence angles of 10^{-7} rad are readily achievable.

6. Conclusion

In this paper, a novel collimation testing method based on the differential grating is proposed. Based on the relationship between the divergence or convergence angle and the phase of moiré fringes, it's feasible to determine whether the collimating light is collimated or not. The experimental results verify that this method has a detectable measurement capability of 10^{-7} rad, which is promising for the practical applications of mini measurement devices and lithography tools [16]–[19].

References

[1] D. E. Silva, "A simple interferometric method of beam collimation," *Appl. Opt.*, vol. 10, no. 8, pp. 1980–1982, Aug. 1971.
[2] S. Yokozeki, K. Patorski, and K. Ohnishi, "Collimation method using Fourier imaging and Moiré techniques," *Opt. Commun.*, vol. 14, no. 4, pp. 401–405, Aug. 1975.
[3] C. Shakher, S. Prakash, D. Nand, and R. Kumar, "Collimation testing with circular gratings," *Appl. Opt.*, vol. 40, no. 8, pp. 1175–1179, Mar. 2001.
[4] D. W. Swift, "A simple Moiré fringe technique for magnification checking," *J. Phys. E.*, vol. 7, no. 3, pp. 164–166, Mar. 1974.
[5] M. P. Kothiyal and R. S. Sirohi, "Improved collimation testing using Talbot interferometry," *Appl. Opt.*, vol. 26, no. 19, pp. 4056–4057, Oct. 1987.
[6] C. W. Chang and D. C. Su, "Collimation method that uses spiral grating and Talbot interferometry," *Opt. Lett.*, vol. 16, no. 22, pp. 1783–1784, Nov. 1991.
[7] A. R. Ganesan and P. Venkateswarlu, "Laser beam collimation using Talbot interferometry," *Appl. Opt.*, vol. 32, no. 16, pp. 2918–2920, Jun. 1993.
[8] K. V. Sriram, M. P. Kothiyal, and R. S. Sirohi, "Collimation testing with linear dual field, spiral and evolute grating: A comparative study," *Appl. Opt.*, vol. 33, no. 31, pp. 7258–7260, Nov. 1994.
[9] D. E. Silva, "Talbot interferometer for lateral and radial derivatives," *Appl. Opt.*, vol. 11, no. 11, pp. 2613–2624, Nov. 1972.
[10] L. Huang and X. Y. Su, "Method for acquiring the characteristic parameter of the dual-spiral Moiré fringes," *Opt. Lett.*, vol. 33, no. 8, pp. 872–874, Apr. 2008.
[11] M. P. Kothiyal, K. V. Sriram, and R. S. Sirohi, "Setting sensitivity in Talbot interferometry with modified gratings," *Opt. Laser Technol.*, vol. 23, no. 6, pp. 361–365, Dec. 1991.
[12] F. Xu, H. Song, and S. L. Zhou, "Fringe pattern analysis for optical alignment in nanolithography using two-dimensional Fourier transform," *Opt. Eng.*, vol. 50, no. 8, pp. 088001-1–088001-7, Aug. 2011.
[13] S. L. Zhou *et al.,* "Fourier-based analysis of Moiré fringe patterns of superposed gratings in alignment of nanolithography," *Opt. Exp.*, vol. 16, no. 11, pp. 7869–7880, May 2008.
[14] S. Zhou, Y. Yang, L. Zhao, and S. Hu, "Tilt-modulated spatial phase imaging method for wafer-mask leveling in proximity lithography," *Opt. Lett.*, vol. 35, no. 18, pp. 3132–3134, Sep. 2010.
[15] S. Zhou *et al.,* "Moiré-based phase imaging for sensing and adjustment of in-plane twist angle," *IEEE Photon. Technol. Lett.*, vol. 25, no. 18, pp. 1847–1850, Sep. 2013.
[16] J. P. Zhu *et al.,* "Four-quadrant gratings Moiré fringe alignment measurement in proximity lithography," *Opt. Exp.*, vol. 21, no. 3, pp. 3463–3473, Feb. 2013.
[17] J. P. Zhu *et al.,* "Influence of tilt Moiré fringe on alignment accuracy in proximity lithography," *Opt. Lasers Eng.*, vol. 51, no. 4, pp. 371–381, Apr. 2013.
[18] J. P. Zhu, J. S. Yu, P. Zhou, and J. Yu, "Experimental study of Talbot imaging moiré-based lithography alignment method," *Opt. Lasers Eng.*, vol. 58, pp. 54–59, Jul. 2014.
[19] J. P. Zhu, J. S. Yu, S. Hu, and Y. Tang, "Alignment method based on matched dual-grating Moiré fringe for proximity lithography," *Opt. Eng.*, vol. 51, no. 11, p. 113603, Nov. 2012.